Quantum nondemolition readout using a Josephson bifurcation amplifier

N. Boulant,[1] G. Ithier,[1,*] P. Meeson,[1,*] F. Nguyen,[1] D. Vion,[1] D. Esteve,[1] I. Siddiqi,[2,†] R. Vijay,[2] C. Rigetti,[2] F. Pierre,[2,‡]
and M. Devoret[2]

[1]*Quantronics Group, Service de Physique de l'Etat Condensé, CEA-Saclay, 91191 Gif-sur-Yvette, France*
[2]*Department of Applied Physics and Physics, Yale University, New Haven, Connecticut 06520-8284, USA*

We report an experiment on the determination of the quantum nondemolition (QND) nature of a readout scheme of a quantum electrical circuit. The circuit is a superconducting quantum bit measured by microwave reflectometry using a Josephson bifurcation amplifier. We perform a series of two subsequent measurements, record their values and correlation, and quantify the QND character of this readout.

PACS number(s): 74.78.-w, 85.25.Cp, 85.25.Am, 03.65.Yz

I. INTRODUCTION

Performing repeated measurements on a single quantum object has become possible with the technological advances of the last 30 years. When the state of the system is destroyed by the measuring apparatus, the quantum object has to be prepared and measured in an identical manner a large number of times so that the ensemble description of the experiment is adequate.[1] It was while developing methods and techniques to detect gravitational waves with accuracy levels exceeding the standard quantum limits[1] that experiments with repeated measurements were first envisioned. It is within this context that the special kind of "quantum nondemolition" (QND) measurement was designed and first coined by Braginsky and Vorontsov in 1975.[2] A QND measurement is defined as a projective measurement where the output state of the measured quantum object is unaffected by subsequent measurements[1,3] and by its free evolution (see mathematical definitions in Sec. IV). When the state, however, is disturbed by the measuring apparatus or by other degrees of freedom during the measurement, one can still quantify the disturbance by measuring the QND "fractions"—i.e., the probabilities of leaving each possible projected state unaffected by the measurement.

Here we report an experiment on a quantum electrical circuit, the quantronium,[4] where the QND fraction left by the readout apparatus—namely, the Josephson bifurcation amplifier (JBA),[5] coupled to a split Cooper pair box—was measured. We first start with a review of the quantronium and its different components. Second, we describe the JBA measurement principles and motivate its QND aspect. We then describe the experimental setup and present the experimental results. Our data and model provide lower bounds on the QND fractions of the JBA in this particular setup.

II. QUANTRONIUM CIRCUIT

The basic element of the quantronium circuit is a split Cooper pair box (Fig. 1). It consists of a low-capacitance superconducting electrode, called the island, connected to a superconducting reservoir by two parallel Josephson junctions with capacitances $C_j/2$ and Josephson energies $E_J(1 \pm d)/2$, where d is the asymmetry factor quantifying the difference between the two junctions $(0 \leq d \leq 1)$,[4,6] E_J

$= \varphi_0 I_0$, I_0 is the sum of the critical currents of the junctions, and $\varphi_0 = \hbar/2e$ is the reduced flux quantum. The island is biased by a voltage source V_{g0} in series with a gate capacitance C_g. The second energy scale of the box is the Coulomb energy $E_{CP} = (2e)^2/2(C_g + C_j)$. For readout purposes, a larger Josephson junction is inserted in the superconducting loop formed by the island, the two junctions, and the reservoir. The quantronium qubit is then described by the Hamiltonian

$$H = E_{CP}(\hat{N} - N_g)^2 - E_j \left(\cos \frac{\delta}{2} \cos \hat{\theta} - d \sin \frac{\delta}{2} \sin \hat{\theta} \right), \quad (1)$$

where $\hat{N}$ is the operator associated with the number of excess Cooper pairs in the island, $N_g = C_g V_{g0}/2e$ is the reduced gate charge, $\hat{\theta}$ is the superconducting phase operator ("conjugate" to $\hat{N}$—i.e., $[\hat{\theta}, \hat{N}] = i$), and δ is the superconducting phase
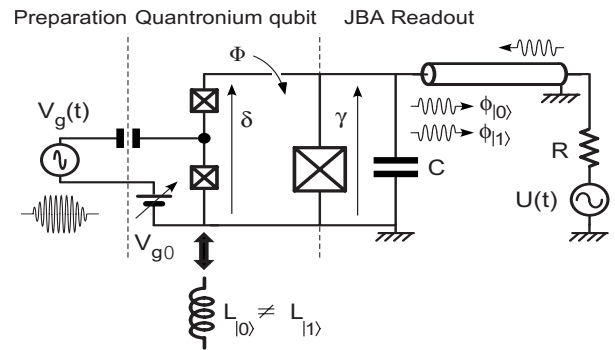

FIG. 1. Quantronium circuit with preparation and readout ports. The qubit consists of two Josephson junctions delimiting an island (black node) and inserted in a superconducting loop. Its eigenstates are tuned using the dc gate voltage V_{g0} and the magnetic flux Φ through the loop. Resonant microwave pulses $V_g(t)$ are applied to the gate to manipulate the qubit state. A larger junction and a shunt capacitor C forming an anharmonic oscillator are inserted in the loop for readout. A microwave readout pulse is sent to the system by a microwave generator with internal impedance $R = 50\ \Omega$. The state-dependent inductive behavior of the qubit affects the plasma resonance of the oscillator and modifies the phase ϕ of the microwave readout pulse reflected by the system. In the case of large driving amplitudes, the dynamics of the superconducting phase γ across the readout junction can bifurcate between two distinct dynamical states, leading to a jump of ϕ.

across the series combination of the two small junctions. Hence this Hamiltonian can be tuned using the N_g and δ control knobs (considered as classical parameters for most applications of interest). For most values of (N_g, δ), the Hamiltonian has a strongly anharmonic energy spectrum, allowing a qubit—i.e., a quantum two-level system—to be encoded into the first two energy levels.[4,6] In addition, by symmetry, the system possesses in this parameter space points where $\partial \nu_{01}/\partial N_g = \partial \nu_{01}/\partial \delta = 0$. At these optimal working points, the qubit is immune to dephasing arising from fluctuations of N_g and δ, up to first order.[7]

III. JOSEPHSON BIFURCATION AMPLIFIER READOUT

To implement a QND readout, we use a dispersive method based on the reflection of a microwave pulse on the parallel combination of the qubit with a nonlinear oscillator made of the readout Josephson junction and an on-chip capacitance. This scheme is called the Josephson bifurcation amplifier[5] (see Fig. 1). Its operating principle relies on the fact that the dynamics of the phase γ across the readout junction depends on the total inductance of the circuit, itself dependent on the qubit state. The phases δ and γ are linked by the relation $\delta = \gamma + \Phi/\varphi_0$, where Φ is the flux threading the quantronium loop. When sending a microwave signal onto the circuit, the classical equation of motion of the phase across the readout junction, assuming the qubit remains in one of the instantaneous qubit eigenstates $|0(\delta(t))\rangle$ or $|1(\delta(t))\rangle$ (adiabatic limit[8]), is

$$RC\varphi_0 \ddot{\gamma} + \varphi_0 \dot{\gamma} + R\left(I_0 \sin \gamma + \frac{1}{\varphi_0}\frac{\partial E_{0,1}}{\partial \delta}\right) = U(t), \qquad (2)$$

where the reader can refer to Fig. 1 to identify the different variables and $E_{0,1}$ denote the energies for the ground and first excited states $|0\rangle$ and $|1\rangle$, respectively. In this paper, the circuit is operated only at $\Phi = 0$, which implies $\delta = \gamma$ and corresponds to an optimal point for $\gamma = 0$. Taylor-expanding eigenenergies to second order yields

$$\frac{\partial E_{0,1}}{\partial \delta} = \underbrace{\frac{\partial E_{0,1}}{\partial \delta}\bigg|_0}_{=0} + \delta \left.\frac{\partial^2 E_{0,1}}{\partial \delta^2}\right|_0 = \delta(\varphi_0^2 L_{0,1}^{-1}), \qquad (3)$$

where $L_{0,1}$ denote the effective qubit inductances corresponding to the states $|0\rangle$ and $|1\rangle$. This scheme therefore constitutes a dispersive measurement in the sense that the second derivative of the energy with respect to δ is measured. For small excursions of the phase γ, the dynamics is the one of a damped harmonic oscillator. As the microwave power is increased, one enters the nonlinear regime of the oscillator. When the detuning of the microwave frequency with respect to the plasma frequency ω_p of the readout junction, $\Delta\omega = \omega_p - \omega$, is such that $\Delta\omega > (\sqrt{3}/2Q)\omega_p$ and when the drive current $U/R > I_B$, where I_B is the bifurcation current given in Ref. 9 and $Q = \omega_p RC$ is the quality factor of the readout junction, the resonator switches from a small-amplitude to a large-amplitude state, these two dynamical states having different phases ϕ of oscillation.[10] This phenomenon has a probabilistic nature in both quantum and thermal regimes. In our experiment, it occurs at the thermal to quantum crossover $k_B T = \hbar\omega_p$,[11] and the frequency and amplitude of the drive current can be tuned so that the system bifurcates with a high (low) probability when the qubit is in state $|1\rangle$ ($|0\rangle$). This bifurcation is detected by measuring the phase ϕ using homodyne demodulation. The method allows single-shot discrimination of the inductances $L_{0,1}$ and hence of the qubit states.

IV. QND CHARACTER OF THE JBA MEASURING THE QUANTRONIUM

When studying a measurement problem quantum mechanically, the total system is often conveniently described with the following Hamiltonian:[1,3,12]

$$H_{tot} = H_S + H_P + H_I, \qquad (4)$$

where H_S, H_P, and H_I are the system, the probe (the measuring apparatus), and their interaction Hamiltonians, respectively. When trying to measure an observable A_S, one should obviously have $\partial H_I/\partial A_S \neq 0$. The standard conditions to have a QND measurement are the following.[3]

(i) $[H_I, A_S] = 0 \Rightarrow$ there is no back action of the measuring device on the measured observable.

(ii) $[H_S, A_S] = 0 \Rightarrow$ a subsequent free evolution after the measurement leaves the projected state of the system unaffected.

After the projection of the first measurement, subsequent free evolutions and measurements always yield the same outcome. When $[H_S, H_I] \neq 0$, determining the basis into which the wave function collapses, the so-called pointer states basis,[12] can be a difficult task. Cucchietti *et al.* indeed show the rotation of that pointer basis with the relative strengths of the system and interaction Hamiltonians in the case of a central spin system coupled to a spin environment.[13] We now show, however, that for the JBA with a low-asymmetry factor d there is no ambiguity in the two-level approximation.

We now write the total Hamiltonian of the quantronium coupled to the readout junction under irradiation:

$$H_{tot} = E_{CP}(\hat{N} - N_g)^2 - E_J\left[\cos(\hat{\theta}) \otimes \cos\left(\frac{\hat{\delta}}{2}\right) - d\sin(\hat{\theta})\right.$$

$$\left. \otimes \sin\left(\frac{\hat{\delta}}{2}\right)\right] + \frac{\hat{Q}^2}{2C} - E_{J0}\cos(\hat{\delta}) - \frac{U(t)}{R}\varphi_0\hat{\delta}, \qquad (5)$$

where E_{J0} is the Josephson energy of the readout junction and $[\varphi_0\hat{\delta}, \hat{Q}] = i\hbar$. Note that the dissipation of the anharmonic oscillator was not included here for the sake of simplicity. The structure of H_{tot} should make the correspondence with Eq. (4) obvious. However, because the coupling between the system and the measuring apparatus is strong—i.e., $E_J \approx E_{CP}$—and because under no irradiation $\langle\cos(\hat{\delta}/2)\rangle \approx 1$, we recast the Hamiltonian as
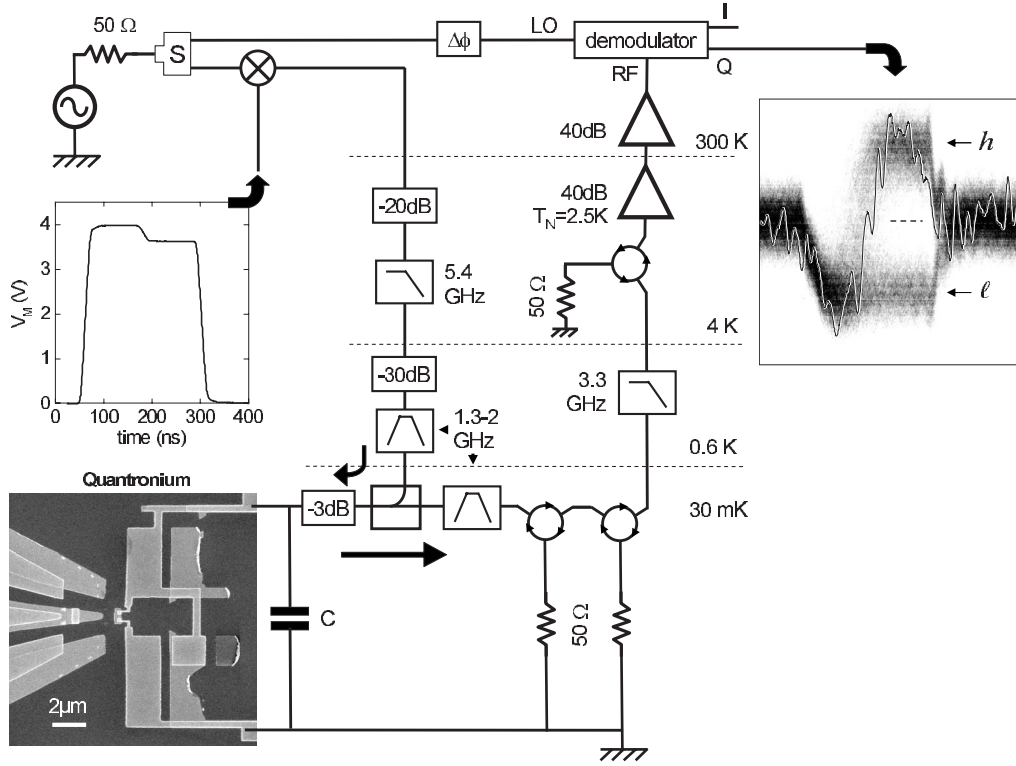
FIG. 2. Experimental setup of the JBA readout. The probing pulses come from the continuous microwave source mixed with a dc pulse $V_M(t)$ (middle left inset), consisting of a first plateau aimed at inducing the bifurcation or not and of a latching period for measuring the phase φ. The resulting microwave pulses propagate to the microfabricated circuit (bottom left SEM micrograph) along a filtered attenuated line and a directional coupler. The reflected pulse travels through the coupler and to the amplification stage via three cascaded circulators. Then it undergoes a homodyne demodulation; one of the quadratures is recorded with respect to time. The top right inset shows in gray levels thousands of superposed records, with one of them emphasized (shaded line). The observed quadrature either follows the envelope of the readout pulse when no bifurcation occurs (bottom traces, readout outcome $r=l$) or switches upwards in the opposite case (readout outcome $r=h$), corresponding to a phase jump. A threshold (dashed line) is used to count the switching events and deduce a switching probability.

$$H_{Tot} = \underbrace{E_{CP}(\hat{N} - N_g)^2 - E_J \cos(\hat{\theta})}_{\text{system Hamiltonian}}$$

$$\underbrace{- E_J \left\{ \cos(\hat{\theta}) \otimes \left[\cos\left(\frac{\hat{\delta}}{2}\right) - 1 \right] - d \sin(\hat{\theta}) \otimes \sin\left(\frac{\hat{\delta}}{2}\right) \right\}}_{\text{interaction Hamiltonian}}$$

$$\underbrace{+ \frac{\hat{Q}^2}{2C} - E_{J0} \cos(\hat{\delta}) - \frac{U(t)}{R} \varphi_0 \hat{\delta}.}_{\text{probe Hamiltonian}} \tag{6}$$

To simplify our analysis, we now restrict ourselves to the first two energy eigenstates of the system, supposed to be biased at the optimum $N_g = 1/2$. With this truncation, the Hamiltonian can be conveniently reexpressed as Eq. (4) with

$$H_S = -\frac{\hbar \omega_{01}}{2} \sigma_z,$$

$$H_I = -\left\{ \alpha \sigma_z \otimes \left[\cos\left(\frac{\hat{\delta}}{2}\right) - 1 \right] - \beta \sigma_y \otimes \sin\left(\frac{\hat{\delta}}{2}\right) \right\},$$

$$H_P = \frac{\hat{Q}^2}{2C} - E_{J0} \cos(\hat{\delta}) - \frac{U(t)}{R} \varphi_0 \hat{\delta}, \tag{7}$$

where $\sigma_{z,y}$ denote the Pauli spin matrices, $\alpha = E_J(\langle 0|\cos \hat{\theta}|0\rangle - \langle 1|\cos \hat{\theta}|1\rangle)/2$, and $\beta = idE_J(\langle 0|\sin \hat{\theta}|1\rangle - \langle 1|\sin \hat{\theta}|0\rangle)/2$. With $A_S = \sigma_z$, the QND conditions are fulfilled in the limit $d=0$. By symmetry, when d is not strictly equal to zero, we expect a correction to the QND fraction of order d^2.

V. MEASURING THE QND FRACTIONS

A. Experimental setup

The sample (see SEM inset of Fig. 2) was fabricated on an oxidized Si chip using standard double-angle evaporation and oxidation of aluminum through a shadow mask patterned by e-beam lithography. The sample was mounted on the cold plate of a dilution refrigerator and wired as indicated in Fig. 2. The JBA setup used at CEA is similar to the one described in Ref. 5. The plasma frequency of the sample was lowered in the $1-2$ GHz bandwidth by adding an on chip capacitor equal to 33 pF in parallel with the junction. It is then easier to control the macroscopic electromagnetic environment in this frequency range than at higher frequencies. Furthermore,

the thermal population of the resonator is still negligible ($\hbar\omega_p/k_B T = 3$). For generating and demodulating the microwave pulses, the output of a microwave generator is split into two channels. One of the channels is used for the homodyne detection of the reflected signal on the system, while the other one is mixed (using Minicircuit ZEM-4300MH mixers) with pulses coming from an arbitrary wave-form generator. The resulting microwave pulses are then sent to the microwave excitation line, which is strongly attenuated in order to use the full dynamical range of the microwave generator, and thus increase the signal-to-noise ratio at the level of the sample. At 30 mK, this line is coupled to the sample through a directionnal coupler (−16 dB coupling) via a 3-dB attenuator to avoid standing waves between the sample and the directional coupler. This main line is strongly filtered (bandwidth of 1.2–1.8 GHz) in order to avoid spurious excitation in the qubit by the external noise. After going through two circulators at 30 mK, the signal is amplified by a cryogenic amplifier (Quinstar L-1.5-30 H) with a noise temperature $T_N = 2.2$ K at 1.5 GHz. A third circulator completes the total isolation of the line to 75 dB which provides a strong attenuation of the room-temperature noise in the bandwidth of interest. A second stage of amplification is required and is provided by an amplifier (Miteq AFS4) placed at room temperature. The amplified signal goes through a bandpass filter (K&L-5BT-1000/2000) centered at a tunable frequency and having a bandwidth of about 100 MHz in order to suppress the main part of the noise generated by the amplifier and which could saturate the demodulation card. This demodulation card (Analog Device AD8347) provides the in-phase and quadrature components of the reflected microwave with respect to the carrier reference. Demodulated signals showing no bifurcation (readout outcome $r=l$) or bifurcation (readout outcome $r=h$) are shown in Fig. 2.

The parameters of the sample, determined by electrical measurements and by spectroscopy of the qubit, were $E_{CP} = 1.12$ K, $E_J = 0.39$ K, $d \leqslant 0.1$, $E_{J0} = 20.3$ K, and $C = 33$ pF, which led to $\alpha \approx 0.2$ K, $\beta \leqslant 0.02$ K, and $\omega_{01}/2\pi \approx 8.1$ GHz. We have coherently manipulated the quantronium state, achieving 55%-contrast Rabi oscillations as opposed to 40% with the dc switching readout scheme previously used.[14,15] The discrepancy between the experimental contrast and the one expected theoretically [≈90% (Ref. 15)] can be partially attributed to spurious relaxation during the readout pulse. Indeed, the ac Stark shift of the qubit due to the applied microwave modifies the transition frequency and can make it cross electromagnetic resonances able to relax the qubit very efficiently.[5]

B. Experimental results

To measure the two QND fractions of the JBA, we prepared the states $|0\rangle$ and $|1\rangle$ in distinct experiments, then sent two successive nominally identical measurement pulses, recorded the switching events for both measurements, and extracted their correlations. The $|1\rangle$ state was prepared by applying a π pulse, whose power and duration were deduced from the analysis of Rabi oscillations, while the $|0\rangle$ state was simply obtained by letting the system relax to the ground
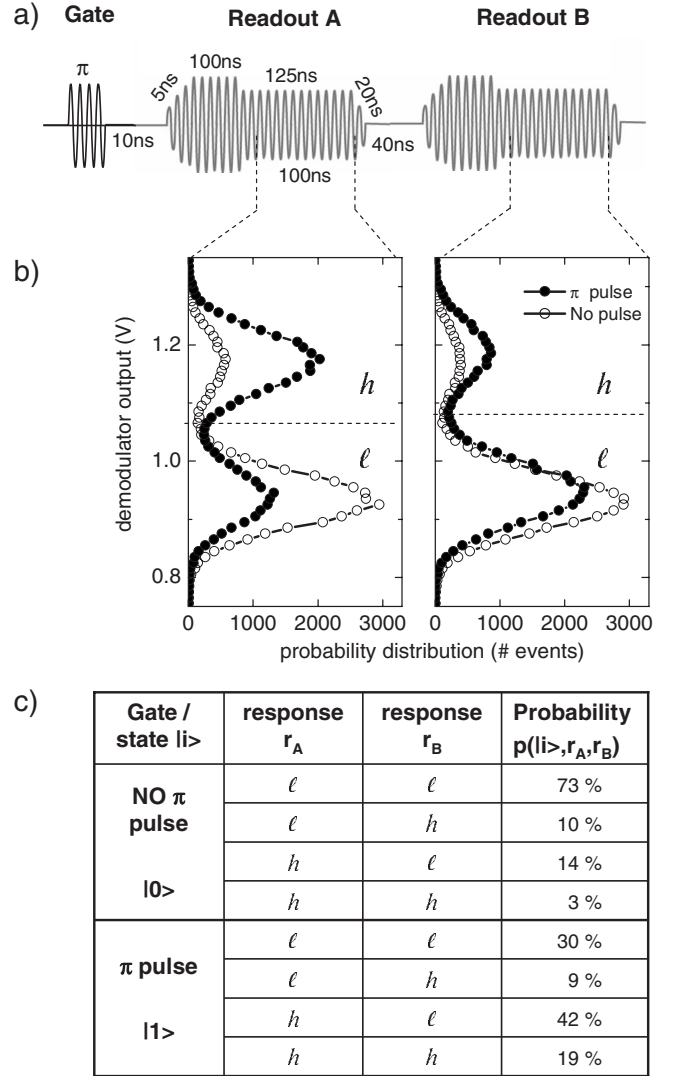

Gate / state $|i\rangle$	response r_A	response r_B	Probability $p(|i\rangle, r_A, r_B)$
NO π pulse **$|0\rangle$**	ℓ	ℓ	73 %
	ℓ	h	10 %
	h	ℓ	14 %
	h	h	3 %
π pulse **$|1\rangle$**	ℓ	ℓ	30 %
	ℓ	h	9 %
	h	ℓ	42 %
	h	h	19 %

FIG. 3. Measurement of the QND fractions of the quantronium-JBA system. Panel (a): the qubit is prepared in state 1 (0) by applying a gate π pulse (no π pulse). Then two adjacent readout pulses A and B are applied. The two successive output quadrature voltages are averaged during the last 100 ns of the latching period of the pulses. Panel (b): bivalued histograms of the quadrature voltages (open symbols, no π pulse; solid symbols, π pulse). The top and bottom peaks correspond to bifurcation (readout $r=h$) and no bifurcation (readout $r=l$), respectively. A threshold (dashed horizontal line) leads to the determination of the bifurcation probabilities. Panel (c): the eight probabilities of getting two successive responses (r_A, r_B).

state. The experiment schematics is provided in Fig. 3. The probabilities $p(|i\rangle, r_A, r_B)$ of the possible outcomes r_A and r_B ($r=l$ or $r=h$) for the two readouts A and B, starting from state $|i\rangle$ ($|0\rangle$ or $|1\rangle$) before readout, were measured over 2×10^4 events [see Fig. 3(c)]. If the readout discrimination between both qubit states was perfect, one could infer the QND fraction directly from the second answer r_B. The situation here, however, is a bit more complex due to the imperfect fidelity of the readout. We thus introduce the probabilities

$$P^A(|i\rangle, r, |f\rangle) \qquad (8)$$

for getting the response r at readout A starting from state $|i\rangle$ before and leaving the qubit in state $|f\rangle$ after. Like the data set p, the probability set P^A contains eight variables constrained by two normalization relations—i.e., six independent variables. We also introduce for both states the probability $P^{A,B}(|i\rangle, r)$ to obtain a given answer, whatever the final state. Although the pulses A and B are nominally identical, the switching rate is so sensitive to small changes of the microwave amplitude a of the readout pulses that it is necessary to introduce a small uncontrolled amplitude difference δa between both pulses. In order to deal with this complication, we have independently measured (data not shown) the derivative of the switching probabilities $\partial P^A(|i\rangle, r=h)/\partial a$, which allows us to evaluate the effect of a small amplitude change. Besides, direct observation of the microwave pulses with an oscilloscope provides an upper bound $|\delta a/a|$ $< 0.5\%$ for such uncontrolled amplitude differences between the two readout pulses. The set of equations linking the probabilities introduced in the model is

$$p(|i\rangle, r_A, r_B) = \sum_{f=0,1} P^A(|i\rangle, r_A, |f\rangle) P^B(|f\rangle, r_B), \qquad (9)$$

where

$$P^B(|f\rangle, r_B) = P^A(|f\rangle, r_B) + \partial P^A(|f\rangle, r_B)/\partial a \, \delta a. \qquad (10)$$

The probabilities $P^A(|i\rangle, r_B)$ are readily obtained from Eq. (9) by summing over the possible outcomes of the second measurement:

$$P^A(|i\rangle, r_A) = \sum_{r_B=l,h} p(|i\rangle, r_A, r_B). \qquad (11)$$

The system to solve is thus a linear system depending on the parameter δa. We find that it yields acceptable solutions—i.e., with positive values in the range $[0,1]$—only for $\delta a/a$ $< -0.4\%$. Taking into account the upper bound already mentioned, $|\delta a/a| < 0.5\%$, and the error bars in the measured probabilities, we obtain the solution given in Fig. 4, which yields the following QND fractions for both qubit states:

$$q_1 = \sum_{r_A=l,h} P^A(|1\rangle, r_A, |1\rangle) = 34\% \pm 2\%, \qquad (12)$$

$$q_0 = \sum_{r_A=l,h} P^A(|0\rangle, r_A, |0\rangle) = 100\% + 0 - 2\%. \qquad (13)$$

The large departure from perfect QND readout observed in this experiment cannot be attributed to the nonzero asymmetry factor $d < 0.1$, which would yield corrections of at most 1%. Besides, our results are to be compared with the ones obtained in similar JBA readout experiments performed on a quantronium at Yale [$q_0 = 100\%$, $q_1 = 55\% \pm 5\%$ (Ref. 16)] and on a flux-qubit at T.U. Delft [$q_0 = 100\%$ and $q_1 > 76\%$ (Ref. 17)]. The difference between the couplings of these two circuits to their environments may explain the differences observed for the QND character and for the readout fidelity. Although the theory in the two-level approximation predicts the JBA measurement to be a QND process, it is clear that during the measurement itself, other environmental
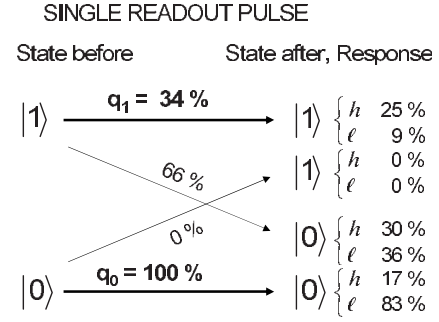

FIG. 4. Readout outputs and qubit state evolution in a measurement by a single readout pulse. The kets $|\psi=0,1\rangle$ indicate the qubit state before (left) and after (right) the measurement. The arrows and their associated probabilities correspond to the different possible qubit evolutions. The QND fractions are indicated in bold. The different readout responses for each different scenario are indicated on the right with their probabilities.

degrees of freedom interact with the system and cause it to relax, thus reducing the contrast of the Rabi oscillations.[7] As a consequence, all we can directly characterize is the combined action of the measurement itself and the environment on the qubit. Whether the JBA scheme itself is fully QND or not can be eventually inferred using additional independent relaxation time, T_1, measurements. Using the T_1 value at the optimal point, one can estimate the QND fraction, correcting for the relaxation that would occur if no readout pulse was applied—i.e., for $\delta = 0$. The zeroth-order loss being $1 - \exp(-t/T_1) = 0.20$, with $T_1 = 1.3$ μs, the corrected QND fraction for state $|1\rangle$ is thus $54\% \pm 2\%$. However, this value must be considered with caution since there is no proof that relaxation during the readout pulse is the same as during free evolution. Indeed, one should bear in mind that T_1 greatly depends on the spectral density of the available states for qubit decay. This density can vary significantly with the qubit frequency,[7] which is changed by the Stark shift due to the ac excitation.[9]

VI. CONCLUSION

We have analyzed and characterized the quantum nondemolition aspect of the JBA readout scheme for the quantronium. For vanishing asymmetry, in the two-level approximation, the theory predicts a QND measurement. We have carried out an experiment consisting of preparing two orthogonal qubit states and then sending a series of two subsequent measurement pulses in order to measure both outcomes and their correlation. Using our model and data, we were able to obtain bounds on the QND fractions of this measurement scheme. The results obtained show that the QND character of the JBA readout of the quantronium is less perfect than expected, but the reasons for this discrepancy are not understood presently. Additional measurements of the T_1 dependence on the control parameters and a better control of the measurement pulse shapes in our experimental setup should lead to a more precise estimation of the QND fractions and of the parameters that affect it.

*Current address: Royal Holloway, Department of Physics, Egham, Surrey, TW20 0EX, UK.

†Present address: Department of Physics, U.C. Berkeley, 94720 California, USA.

‡Present address: LPN, Route de Nozay, 91460 Marcoussis, France.

[1] V. B. Braginsky and F. Ya. Khalili, *Quantum Measurement* (Cambridge University Press, Cambridge, England, 1992).

[2] V. B. Braginsky and Yu I. Vorontsov, Sov. Phys. Usp. **17**, 644 (1975).

[3] M. O. Scully and M. S. Zubairy, *Quantum Optics* (Cambridge University Press, Cambridge, England, 1997).

[4] D. Vion, A. Aassime, A. Cottet, P. Joyez, H. Pothier, C. Urbina, D. Esteve, and M. H. Devoret, Science **296**, 886 (2002).

[5] I. Siddiqi, R. Vijay, F. Pierre, C. M. Wilson, M. Metcalfe, C. Rigetti, L. Frunzio, and M. H. Devoret, Phys. Rev. Lett. **93**, 207002 (2004); I. Siddiqi, R. Vijay, M. Metcalfe, E. Boaknin, L. Frunzio, R. J. Schoelkopf, and M. H. Devoret, Phys. Rev. B **73**, 054510 (2006).

[6] A. Cottet, Ph.D. thesis, Université Paris VI, 2002 [available at http://tel.ccsd.cnrs.fr (in English)].

[7] G. Ithier, E. Collin, P. Joyez, P. J. Meeson, D. Vion, D. Esteve, F. Chiarello, A. Shnirman, Y. Makhlin, J. Schriefl, and G. Schon, Phys. Rev. B **72**, 134519 (2005).

[8] This assumption is valid as long as the qubit transition frequency is large compared to the driving frequency, which is the case here.

[9] I. Siddiqi, R. Vijay, F. Pierre, C. M. Wilson, L. Frunzio, M. Metcalfe, C. Rigetti, and M. H. Devoret, arXiv:cond-mat/0507248 (unpublished).

[10] L. D. Landau and E. M. Lifchitz, *Mechanics* (Reed, Oxford, 1981).

[11] M. I. Dykman, Phys. Rev. E **75**, 011101 (2007).

[12] W. H. Zurek, Phys. Rev. D **24**, 1516 (1981); **26**, 1862 (1982).

[13] F. M. Cucchietti, J. P. Paz, and W. H. Zurek, Phys. Rev. A **72**, 052113 (2005).

[14] E. Collin, G. Ithier, A. Aassime, P. Joyez, D. Vion, and D. Esteve, Phys. Rev. Lett. **93**, 157005 (2004).

[15] G. Ithier, Ph.D. thesis, Université Paris VI, 2005 [available at http://tel.ccsd.cnrs.fr (in English)].

[16] R. Vijay (unpublished).

[17] A. Lupascu, S. Saito, T. Picot, P. C. de Groot, C. J. P. M. Harmans, and J. E. Mooij, Nat. Phys. **3**, 119 (2007).